EBioMedicine 2 (2015) 214–224

Contents lists available at ScienceDirect

EBioMedicine

journal homepage: www.ebiomedicine.com

Original Article

Soluble CLEC2 Extracellular Domain Improves Glucose and Lipid Homeostasis by Regulating Liver Kupffer Cell Polarization

Xinle Wu [a,1], Jun Zhang [a,1], Hongfei Ge [a], Jamila Gupte [a], Helene Baribault [a], Ki Jeong Lee [b], Bryan Lemon [a], Suzanne Coberly [a], Yan Gong [a], Zheng Pan [a], Ingrid C. Rulifson [a], Jonitha Gardner [a], William G. Richards [b], Yang Li [a,*]

[a] Amgen Inc., 1120 Veterans Blvd., South San Francisco, CA 94080, United States
[b] Amgen Inc., One Amgen Center Drive, Thousand Oaks, CA 91320, United States

ARTICLE INFO

Article history:
Received 30 October 2014
Received in revised form 17 February 2015
Accepted 22 February 2015
Available online 25 February 2015

Keywords:
CLEC2
Macrophage
Kupffer cell
Inflammation
Diabetes
Dyslipidemia

ABSTRACT

The polarization of tissue resident macrophages toward the alternatively activated, anti-inflammatory M2 phenotype is believed to positively impact obesity and insulin resistance. Here we show that the soluble form of the extracellular domain (ECD) of C-type lectin-like receptor 2, CLEC2, regulates Kupffer cell polarization in the liver and improves glucose and lipid parameters in diabetic animal models. Over-expression of Fc-CLEC2(ECD) in mice via in vivo gene delivery, or injection of recombinant Fc-CLEC2(ECD) protein, results in a reduction of blood glucose and liver triglyceride levels and improves glucose tolerance. Furthermore, Fc-CLEC2(ECD) treatment improves cytokine profiles and increases both the M2 macrophage population and the genes involved in the oxidation of lipid metabolism in the liver. These data reveal a previously unidentified role for CLEC2 as a regulator of macrophage polarity, and establish CLEC2 as a promising therapeutic target for treatment of diabetes and liver disease.

1. Introduction

Chronic inflammation is thought to contribute to the development of obesity and metabolic syndromes (Hotamisligil, 2006; Shoelson et al., 2006). Aberrant pro-inflammatory immune responses are found in many organs of diabetic individuals, including the pancreas, liver, adipose, heart, brain, and muscle (Lumeng and Saltiel, 2011). For example, many pro-inflammatory proteins, including TNF-α, interleukin 6 (IL-6) and inducible nitric oxide synthase, secreted from adipose tissue macrophages (ATM), are found at higher levels in adipose tissue from obese individuals compared to lean individuals (Harkins et al., 2004; Hotamisligil, 2006). Increased adiposity promotes macrophage infiltration and local inflammation, which in turn contributes to increasing insulin resistance (Weisberg et al., 2003; Xu et al., 2003). Inflammatory responses in the liver, another major metabolic organ, have also been implicated in obesity, type 2 diabetes and fatty liver diseases. Activation of the resident macrophages in the liver, Kupffer cells, induces hepatotoxicity in obese mice (Li and Diehl, 2003) and regulates hepatic glucose metabolism and insulin resistance (Huang et al., 2010; Lanthier et al., 2010).

Macrophages are derived from monocyte precursors and undergo specific differentiation and activation depending on the local tissue environment and cytokine milieu (Steinman and Idoyaga, 2010). Two distinct states of polarized activation for macrophages have been defined: the classically activated macrophage phenotype, M1, and the alternatively activated macrophage phenotype, M2 (Gordon and Taylor, 2005; Mantovani et al., 2002). M1 macrophages are effector cells in T_H1 cellular immune responses, whereas M2 macrophages appear to promote immune suppression and wound healing/tissue repair (Gordon and Taylor, 2005; Mantovani et al., 2002). Recent evidence demonstrates that in lean animals, higher numbers of macrophages are M2 polarized, possessing anti-inflammatory potential by producing IL-10, while obesity drives pro-inflammatory M1 polarization (Lumeng et al., 2007a,b; Mjosberg et al., 2011). Thus, the M1/M2 switch may occur within local tissues such as fat and liver (Kang et al., 2008; Odegaard et al., 2008), and the balance between M1 and M2 macrophages contribute to the onset of insulin resistance (Charo, 2007; Lumeng et al., 2007a,b). Locally produced T_H2-type cytokines, such as IL-4 and IL-13, and activation of peroxisome proliferator-activated receptor δ/β (PPARδ/β) or PPARγ, result in the activation of M2 macrophages. Disruption of either PPARδ/β or PPARγ in myeloid cells may impair the alternative activation of M2 macrophages in the adipose tissue and liver, resulting in impaired glucose tolerance and exacerbated insulin resistance under high fat diet conditions (Hevener et al., 2007; Kang et al., 2008; Odegaard et al., 2007, 2008).

C-type lectin-like receptor 2 (CLEC2) was initially identified through a computational approach searching for sequences similar to known

* Corresponding author.
E-mail address: yangl@amgen.com (Y. Li).
[1] XW and JZ contributed equally to this work.

http://dx.doi.org/10.1016/j.ebiom.2015.02.013

C-type lectin-like receptors expressed on immune cells (Colonna et al., 2000). CLEC2, a member of the type II transmembrane C-type lectin-like receptor family, has a single YXXL/hemi-ITAM (immuno-receptor tyrosine-based activation motif) within its cytoplasmic domain. Expression of CLEC2 has been detected on the surface of platelets and a number of different immune cells, including dendritic cells, neutrophils, and Kupffer cells (Colonna et al., 2000; Mourao-Sa et al., 2011; Tang et al., 2010). The gene encoding CLEC2 is located in a genetic locus proximal to a distinct cluster of related receptors, including CLEC7A, LOX-1 and CLEC9A; most of which are expressed in myeloid populations (Sobanov et al., 2001).

The first identified ligand for CLEC2 was rhodocytin, a toxin from snake venom that induces platelet aggregation (Hooley et al., 2008; Suzuki-Inoue et al., 2006). More recently, podoplanin, a membrane glycoprotein, was proposed as an endogenous ligand for CLEC2 (Christou et al., 2008; Kato et al., 2008; Suzuki-Inoue et al., 2007). The interaction between CLEC2 and podoplanin is critical for the separation of blood and lymphatic vessels during embryonic development and during some pathophysiological conditions, such as tumor metastasis (Bertozzi et al., 2010). The interaction between the two proteins during embryogenesis is exemplified by the finding that mice deficient for CLEC2 display a similar phenotype as mice deficient for podoplanin, including bleeding and defects in vascular connections. However, in the normal adult state, while CLEC2 is predominantly expressed on cells located within blood vessels, podoplanin is expressed on cells lining lymphatic vessels (Suzuki-Inoue et al., 2007) and thus interaction between the two is unlikely. Therefore, it is possible that other, yet unidentified CLEC2 ligands may exist.

Besides playing a role in platelet aggregation (Chang et al., 2010; Kerrigan et al., 2009; Mourao-Sa et al., 2011), a function for CLEC2 on other immune cells has yet to be defined. Here we show that soluble CLEC2 regulates Kupffer cell polarization in the liver and improves glucose and lipid parameters in diabetic animals, thus revealing a novel physiological role for CLEC2 in both inflammation and metabolism. Our results demonstrate a previously unknown connection between CLEC2 and glucose and lipid metabolism, and support CLEC2 as a potential target for treating diabetes.

2. Materials and Methods

2.1. Fc-CLEC2(ECD)

To design a stable soluble CLEC2 protein that may block endogenous CLEC2 activity, the C-terminal extracellular domain of murine CLEC2 (51-229) was fused with a human Fc protein at its N-terminus connected by a flexible glycine linker (G4SG4), yielding Fc-CLEC2(ECD). DNA vectors for hydrodynamic injection, recombinant AAV preparation and recombinant protein expression all carry the same coding sequence for this Fc-CLEC2(ECD) protein. Recombinant Fc-CLEC2(ECD) was expressed through transient transfection of HEK293 cells and purified via Protein A affinity chromatography.

2.2. Animal Studies

All animal experiments were approved by the Institutional Animal Care and Use Committee of Amgen and cared for in accordance to the *Guide for the Care and Use of Laboratory Animals*, 8th Edition (National Research Council (U.S.). Committee for the Update of the Guide for the Care and Use of Laboratory Animals. et al., 2011). Mice were housed in an air-conditioned room at 22 ± 2 °C with a 12 hour light and 12 hour darkness cycle (0600–1800 h). Mice were randomized into control and treatment groups to achieve similar baseline levels of body weight, fasting glucose and insulin levels. No animals were excluded from the statistical analysis, and data collection was blinded in the studies.

The efficacy of recombinant Fc-CLEC2(ECD) protein was tested in 14-week-old, male B6D2F1/J mice (The Jackson Laboratory) fed for at least 8 weeks with a 60% fat diet, D12492 (Research Diet). The mice received intraperitoneal injection of Fc-CLEC2(ECD) protein diluted in 0.2 ml PBS. The control group received intraperitoneal injections of PBS. Injections were performed 1 to 2 h prior to the dark phase of the light cycle except on days when oral glucose tolerance test (oGTT) was performed. Proteins were then administered 2–3 h before fasting glucose measurement.

Hydrodynamic Tail Vein (HTV) studies were carried out in 12-week-old male B6D2F1/J mice (The Jackson Laboratory) fed with a 60% high fat diet for 6 weeks. Mice were randomized in respective groups based on body weight and both fasting (4 h) blood glucose and serum insulin levels, all of which measured the day before HTV injection. An endotoxin free DNA construct expressing Fc-CLEC2(ECD) was diluted in a saline solution to the concentration of 8 μg/ml. The injection volume was calculated based on body weight, approximately 100 ml/kg, but never exceed 2.5 ml per animal. The DNA solution was injected into the tail vein of mice within a 5–8 second timeframe. The construct carrying human Fc protein alone was used as a negative control.

Recombinant adeno-associated virus (rAAV) expressing Fc-CLEC2(ECD) was produced by transient transfection into 293T cells using the helper-free system, purified by gradient centrifugation, buffer exchanged. Mice were injected through the tail vein with 2–8 × 10^{12} virus particles per mouse of either Fc-CLEC2(ECD), or an empty vector (EV) as the negative control, in PBS.

An oGTT was performed after 4 h of fasting. Mice were injected with a bolus of glucose (10 ml/kg body weight of 20% glucose) into the stomach by a gavage needle (20 G × 1.5 in.) (Popper and Sons). Blood glucose levels were measured with a glucometer from tail tip blood collected at 0, 20, 40, 60, and 90 min after glucose dosing. Serum insulin levels were measured using a mouse insulin ELISA kit (ALPCO Diagnostics). The assay was performed as described by the manufacturer's protocol.

Hepatic triglyceride content was determined using homogenized liver extracts using chloroform/methanol (2:1 v/v) and lysed using a Qiagen tissue lyzer for 30 s to 1 min. Samples were first transferred to 12 × 75 mm glass test tubes and incubated at room temperature for 30–45 min. Samples were then washed with 50 mM NaCl, vortexed, centrifuged at 1500 *g* for 10 min and the organic phase was removed and placed into a new glass tube. The organic phase was washed twice with 0.36 M $CaCl_2$/methanol and centrifuged at 1500 *g* for 10 min. The triglyceride levels were measured using an Infinity triglyceride assay kit (Thermo Scientific).

Serum cytokine measurements were performed using the Bio-Plex Pro cytokine multiplex assay (BioRad) to measure the levels of cytokines in serum samples. Samples were diluted 2-fold in Bio-Plex sample diluent for the assay. The assay was performed according to the manufacturer's protocol. Plates were read on a Bio-Plex system and data was obtained using Bio-Plex Manager software.

2.3. H&E Staining and Immunohistochemistry

All collected tissues were fixed in 10% Neutral Buffered Formalin (NBF) for 24 h, processed to paraffin blocks, and cut into 4 micron sections. The sections were dried overnight in a 37 °C oven, followed by 1 hour incubation in a 60 °C oven prior to deparaffinization. Deparaffinization and H&E staining (Surgipath, Buffalo Grove, IL, USA) were performed on an automated multistainer (Leica ST 5020, Buffalo Grove, IL, USA). The F4/80 antibody, an IgG2b affinity purified rat monoclonal antibody, was purchased from AbD Serotec. The α smooth muscle actin antibody was purchased from Abcam. Morphometric analysis was performed using a Scan Scope XT (Aperio) and both Image Scope (Aperio) and Indica Lab (Indica Lab) software. For each animal, nine 3.6 × 10^5 μm^2 areas were evaluated for the percent F4/80 positive staining per area of tissue.

2.4. Human Fc ELISA

Microtiter plates were coated with 1.0 μg/ml of goat anti-human Fc (Jackson ImmunoResearch) in PBS overnight at 4 °C, and washed one time with PBS. The plates were then blocked with 3% BSA in PBS over night at 4 °C, and washed one time with PBS. Serum samples were diluted in PBS + 1% BSA and incubated for 1 h at room temperature and washed 3 times with PBS + 0.01% Tween-20. Goat anti-human Fc-HRP (Jackson ImmunoResearch) in PBS + 1% BSA was added and incubated for 1 h at room temperature. The plates were washed 6 times with PBS + 0.01% Tween-20 and developed with tetramethyl benzidine (TMB) as substrate. 1 N HCl was added as the stop solution. The results were read on a SpecMax plate reader at 450 nm. Recombinant human Fc protein (Jackson ImmunoResearch) was used for standard curve.

2.5. Macrophage Isolation

Resident peritoneal macrophages were extracted from 6–10-week-old C57BL/6 mice and incubated at 37 °C for 2 h prior to stimulation. Thioglycolate-elicited macrophages were prepared by injecting 2-month-old C57BL/6 mice with 2 ml 3% aged thioglycolate media. On day 4, cells were isolated by and prepared for resident macrophages.

2.6. Quantitative RT-PCR (RT-qPCR)

Human and mouse tissue total RNAs were purchased from Clontech, BioChain Institute, Inc. and Agilent Technologies. Mouse total RNA from hepatocytes and liver non-parenchymal cells was obtained from Zen-Bio. Other tissue or Cell Total RNA was isolated using QIAcube and RNeasy kit (Qiagen). Reaction mixtures contained 100 ng of isolated total RNA, 200 nM of each gene specific primer and probe and Brilliant II QRT-PCR Master mix (Stratagene) in a total volume of 50 μl. All of the reactions were performed in duplicate on a Stratagene MX3000p sequence detection system, and relative mRNA levels were calculated by the comparative threshold cycle method using GAPDH as the internal control.

2.7. Cell Cultures and In Vitro Assays

RAW 264.7 cells were grown in Dulbecco's modified Eagle's medium (DMEM) containing 10% fetal bovine serum and 50 μg/ml streptomycin and penicillin. RAW 264.7 cells were treated with LPS and IL-4 (Sigma) at a concentration of 100 ng/ml for 24 h prior to harvest.

The platelet aggregation assay was performed on a Chrono-log Aggregometer. Platelet- rich plasma (PRP) was analyzed in the presence of either rhodocytin, CLEC2 antibody (Abcam), or with Fc-CLEC2 (ECD). To prepare PRP, fresh whole blood collected from mice was mixed with 10% ACD (Acid-Citrate-Dextrose) buffer (Sigma) and centrifuged at 100 *g* for 20 min. PRP was collected from the top layer.

For Kupffer cell/primary hepatocyte co-culture, Kupffer cells from 12–14 week old male C57BL/6 mice (The Jackson Laboratory) were purchased from Cell Specific (Berkeley, California). Primary hepatocytes were isolated and cultured using Invitrogen liver media and reagents. In brief, animals were CO_2 treated for 2 min until no detectable breathing and pinned down with needles. After opening the abdomen, a 16G catheter was gently inserted into the portal vein and, simultaneously, the interior vena cava vein was severed with scissors. The liver was perfused with 30 ml of pre-warmed perfusion media, followed by 30 ml of liver digestion media. After perfusion, the liver was removed and rinsed with washing media. Forceps were used to peel off the liver capsule and gently shake out hepatocytes. Hepatocytes were filtered through 100 μm cell strainer into a 50 ml conical tube and then washed 3 times by centrifugation at 500 rpm for 3 min to remove the washing media. Primary hepatocytes and Kupffer cells were mixed at a 2:1 ratio in M199 culture media and 4×10^5 cells per well were plated into 6-well plates and incubated at 37 °C. After 48 h, 100 ng/ml of Fc-CLEC2(ECD) or control was mixed with fresh M199 culture media and added to the cells. After a 5 hour incubation, cells were harvested for RNA isolation and RT-qPCR studies.

3. Results

3.1. In Vivo Overexpression of Fc-CLEC2(ECD) Improves Glucose Homeostasis and Attenuates Hepatic Steatosis

During a quest to identify potential novel regulators of metabolism, we noted the relatively high expression levels of *CLEC2* in human liver samples among a panel of tissues examined (Fig. 1A). *Clec2* is also expressed in the mouse liver tissue although the relative level to other tissues is not as high as in humans (Fig. 1B). Fractionation of cells recovered from mouse liver revealed that *Clec2* was highly expressed specifically in non-parenchymal cells compared to hepatocytes (Fig. 1C), consistent with the detection of CLEC2 on Kupffer cells (Tang et al., 2010). As liver plays major roles in the metabolic control of lipid, glucose, and energy metabolism, we wondered if CLEC2 could affect metabolism. Since no soluble ligands have been identified for CLEC2, we took the approach to overexpress a soluble form of CLEC2, which could potentially act as a decoy antagonistic receptor as a way to study CLEC2 function. To achieve a stable and high level expression of CLEC2, the extracellular domain of murine CLEC2 (residues 51–229) was fused with human Fc to generate Fc-CLEC2(ECD) (Fig. 2A). Purified recombinant Fc-CLEC2(ECD) can bind to the known ligand, rhodocytin, and block rhodocytin-induced platelet aggregation in vitro (Fig. 2B and C), demonstrating that this form of CLEC2 is functional. A DNA expression construct carrying Fc-CLEC2(ECD) was delivered in vivo through HTV injection in a diet induced obesity (DIO) mouse model. 12-week-old male B6D2F1/J DIO mice were randomized into two groups based on body weight and baseline glucose levels. The mice in the treatment group were injected with the HTV Fc-CLEC2(ECD) DNA construct and mice in the control group were injected with a DNA construct carrying Fc alone. The expression of full length Fc-CLEC2(ECD) protein was confirmed by Western blot using an anti-human Fc antibody (data not shown). Serum exposure was quantitated by ELISA and revealed that high levels of protein exposure were achieved after HTV delivery (Fig. 2D). Fc-CLEC2(ECD) did not induce significant changes to body weight during the experiment period (Fig. 2E), while a significant reduction in fasting blood glucose levels was observed 13 days after Fc-CLEC2(ECD) treatment (Fig. 2F). At day 13, an oGTT demonstrated a significant improvement in the animals expressing Fc-CLEC2(ECD) compared to the mice in the control group (Fig. 2G). Furthermore, mice in the treatment group also had significantly lowered serum insulin levels (Fig. 2H), suggesting an improvement in insulin sensitivity. Because hepatic steatosis is commonly associated with obesity and diabetes, livers were collected from the mice at day 18 for triglyceride (TG) measurement. Liver TG levels were significantly reduced in the treatment group compared to the control mice (Fig. 2I). No signs of fibrosis were found in livers from either group as indicated by the negative immunohistochemical staining for α smooth muscle actin (αSMA) (Supplementary Fig. 1A). Histopathological analysis of multiple organs, including the liver, lymph node, pancreas, skeletal muscle, spleen, and white fat, also did not reveal any gross abnormalities in mice from either group (data not shown).

3.2. Fc-CLEC2(ECD) Treatment Increases M2 Macrophage Expression in the Liver

To understand the mechanism leading to the improved glucose and lipid profiles post Fc-CLEC(ECD) treatment, since endogenous *Clec2* is highly expressed in the liver, we performed microarray analysis to compare gene expression profiles between livers from the Fc-CLEC2(ECD) treatment group and the control group. Expression analysis revealed

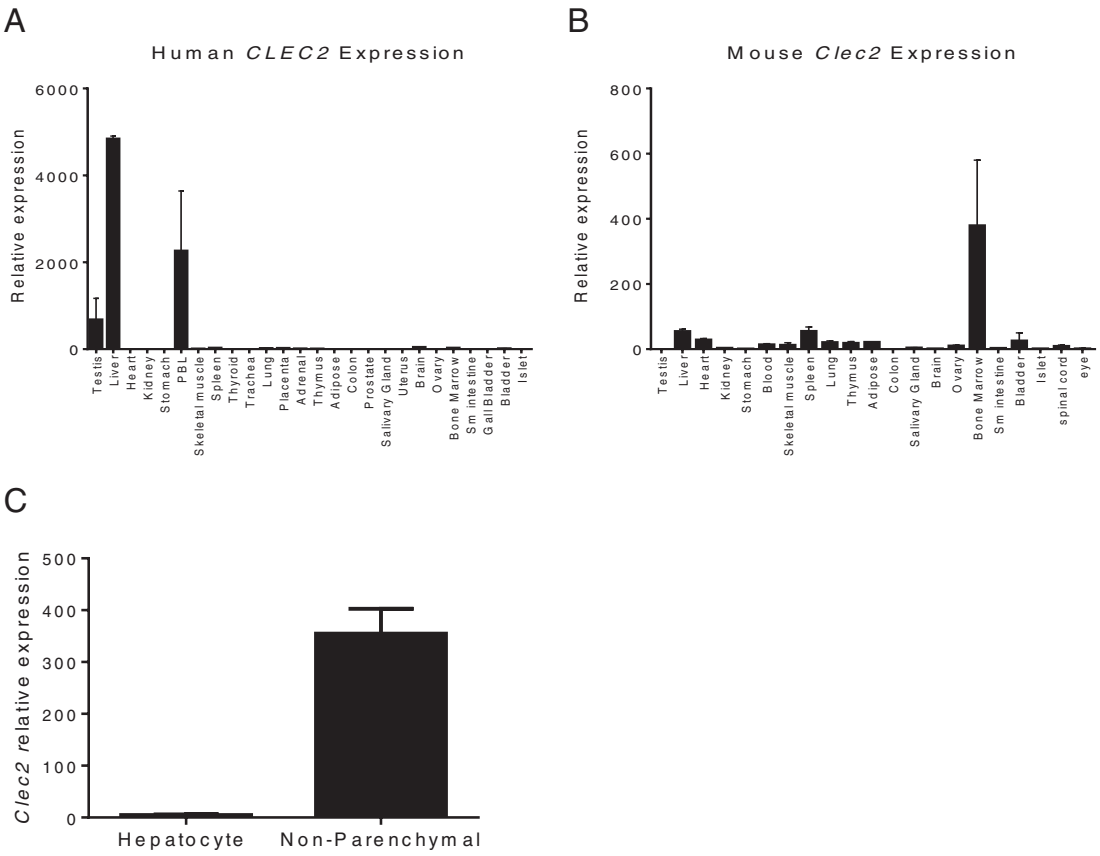

Fig. 1. High expression of *Clec2* in the non-parenchymal fraction of liver cells. (A) RT-qPCR of different human tissues shows *CLEC2* enrichment in the testis, liver and PBL. (B) RT-qPCR of different mouse tissues. (C) *Clec2* is highly expressed in non-parenchymal cells of liver compared to hepatocytes. Results are expressed as the mean ± SEM of triplicates and are representative of two independent experiments.

that the most regulated genes following treatment included many macrophage marker genes. Further confirmed by RT-qPCR analysis, markers of M2 macrophage activation such as *Clec7a* (the gene encoding Dectin-1), *Chi3l3* (the gene encoding Ym-1), and *Retnla* (the gene encoding Fizz-1) were highly induced in the Fc-CLEC2(ECD) treatment group while markers of M1 macrophages such as *Tnfα*, *Il6*, and *iNos* were not significantly changed (Fig. 2J). The induction of M2 markers appeared to be liver specific as no significant changes were observed in the adipose tissue (Supplementary Fig. 2). Immunohistochemical analysis with the macrophage marker, F4/80, in the liver was subsequently performed. This analysis revealed an almost two-fold increase in the F4/80+ staining area of Fc-CLEC2(ECD)-treated mice versus control mice (Fig. 2K and L), which could be due to either an increase in macrophage size and/or number. We also observed the Kupffer cells in the treatment group to be more widely distributed throughout the sinusoids, with an increase in plump cells and clusters around degenerating hepatocytes compared to control mice (Fig. 2K).

3.3. In Vivo Overexpression of Fc-CLEC2(ECD) Delivered by rAAV Improves Glucose Homeostasis

Since the method of HTV injection can induce acute hyper perfusion in the liver, in order to rule out that the observed changes in Kupffer cells were not due to, or enhanced because of the HTV treatment, we used rAAV to overexpress Fc-CLEC2(ECD). B6D2F1/J-DIO mice were injected with either rAAV expressing Fc-CLEC2(ECD) or rAAV containing an empty vector (EV) as the negative control. Similar to the HTV results, no obvious body weight difference between the two groups was detected during the experiment period (Fig. 2M), while mice injected with Fc-CLEC2(ECD) demonstrated significant improvements in oGTT (Fig. 2N) and lower serum insulin levels (Fig. 2O) compared to the control group. The effects of Fc-CLEC2(ECD) in the leptin deficient *ob*/*ob* mouse model were also performed. Six-week-old male *ob*/*ob* mice injected with Fc-CLEC2(ECD) did not exhibit any significant body weight difference compared to control mice (Fig. 2P), while they had lower fasting glucose levels (Fig. 2Q) and showed an improvement in the oGTT (Fig. 2R). In sum, the overexpression of Fc-CLEC2(ECD) using rAAV led to improved glucose homeostasis in two different mouse models; these results are consistent with those observed when HTV was used as a gene delivery method.

3.4. Recombinant Fc-CLEC2(ECD) Protein Improves Glucose and Lipid Homeostasis

Overexpressing Fc-CLEC2(ECD) using the two in vivo gene delivery methods revealed a novel function for CLEC2 in regulating glucose homeostasis. Since both HTV and rAAV drive the expression of the gene-of-interest mainly from the liver, we next wanted to address whether injection of recombinant Fc-CLEC2(ECD) proteins could achieve similar metabolic phenotypes, and thereby establish recombinant Fc-CLEC2(ECD) as a potential therapy to treat diabetes. Thus, 12-week-old male B6D2F1/J-DIO mice were injected with 10 mg/kg or 30 mg/kg of recombinant Fc-CLEC2(ECD) protein or PBS daily. Over the course of two weeks no apparent body weight differences were observed among cohorts (Fig. 3A). However, groups treated with Fc-CLEC2(ECD) manifested either trended (10 mg/kg group) or statistically significant lowering (30 mg/kg group) in plasma insulin levels compared to the PBS control group (Fig. 3B). Similar to the HTV and rAAV studies, both recombinant Fc-CLEC2(ECD) protein treatment groups exhibited significantly improved glucose tolerance compared to the control group (Fig. 3C). Both serum TG levels (Fig. 3D) and liver TG content (Fig. 3E) were lower in groups treated with recombinant Fc-CLEC2(ECD) proteins,

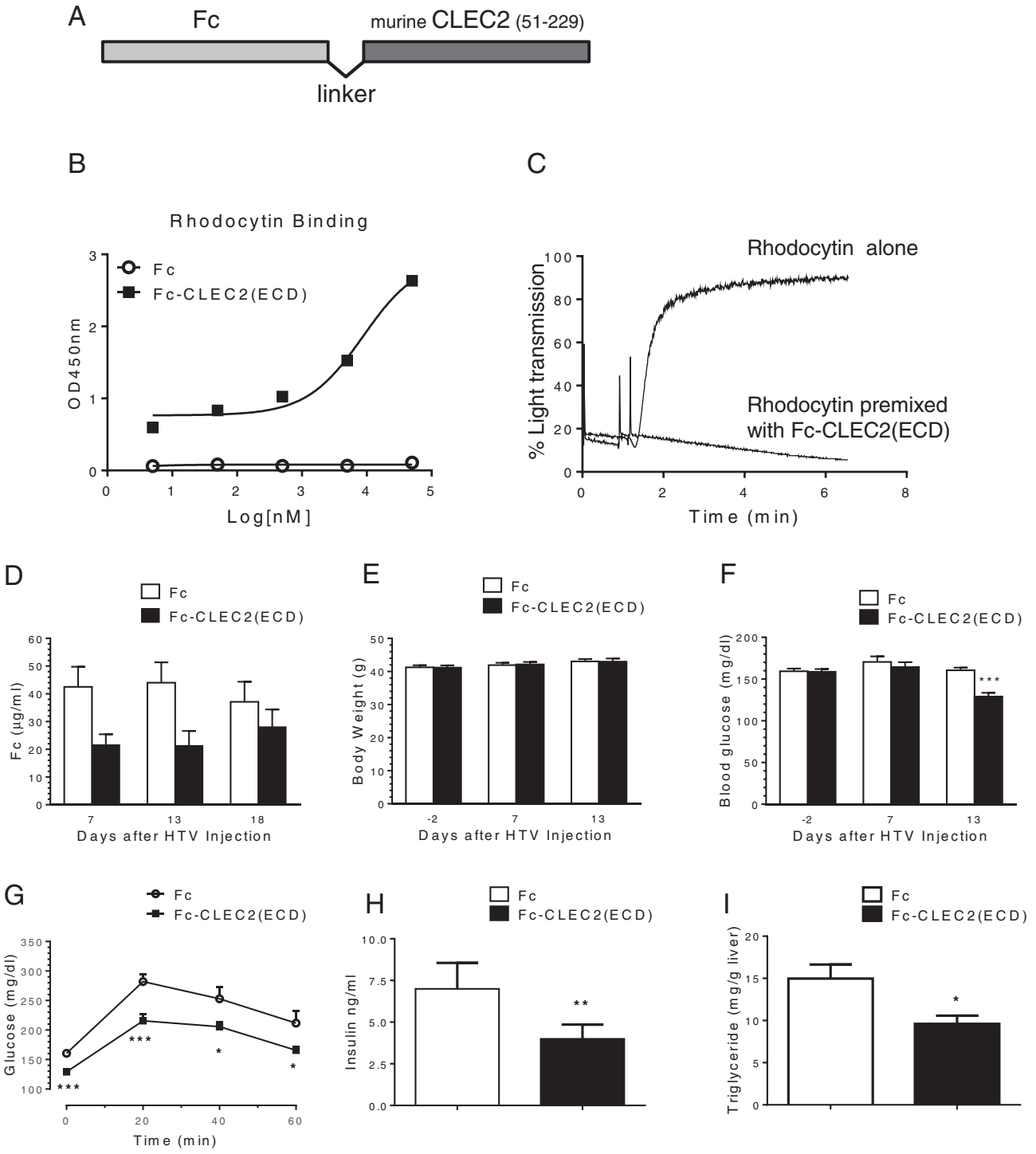

Fig. 2. Improved glucose and lipid homeostasis after over-expression of Fc-CLEC2(ECD) through in vivo gene delivery. (A) Schematic showing the design of Fc-CLEC2(ECD) molecule. (B–C) Purified recombinant Fc-CLEC2(ECD) binds to rhodocytin and blocks rhodocytin induced platelet aggregation. (B) Dose-dependent binding of Fc-CLEC2(ECD) incubated with rhodocytin (50 nM). (C) Fc-CLEC2(ECD) completely blocks rhodocytin-induced platelet aggregation. (D–L) Over-expression of Fc-CLEC2(ECD) through hydrodynamic tail vein gene delivery. (D) Serum levels of Fc-CLEC2(ECD) protein determined by ELISA 7, 13 and 18 days after HTV injection. (E) Body weight comparison between the treatment group and the control group. (F) Fasting serum glucose level is reduced in Fc-CLEC2(ECD) treatment group. (G) Fc-CLEC2(ECD) treatment group shows improvement in glucose tolerance 13 days after HTV injection. (H) Fc-CLEC2(ECD) reduces serum insulin concentration. (I) Liver triglyceride content is reduced from Fc-CLEC2(ECD) group. (n = 15) (J–L) Characterization of liver macrophages after over-expression of Fc-CLEC2(ECD) through HTV delivery (J) Liver gene expression analysis measured by RT-qPCR. (K) Liver macrophage F4/80 staining showing a wider distribution of plump, clustered Kupffer cells in the treated animals, as indicated by arrows. (L) Quantification of liver macrophage F4/80 staining shows increased F4/80 + staining in the Fc-CLEC2(ECD) treatment group. Fc control (n = 10), CLEC2 (n = 9). (M–R) Improved glucose and insulin parameters after over-expression of Fc-CLEC2(ECD) delivered through rAAV. (M) Body weight comparison between DIO mice injected with rAAV expressing Fc-CLEC2(ECD) and control rAAV. (N) DIO mice injected with Fc-CLEC2(ECD) show improvement in glucose tolerance at 23 days after the rAAV injection. (O) Fc-CLEC2(ECD) reduced serum insulin levels in DIO mice. (P) Body weight comparison between *ob*/*ob* mice injected with rAAV expressing Fc-CLEC2(ECD) and control rAAV. (Q) Fasting serum glucose level is reduced in Fc-CLEC2(ECD) treated *ob*/*ob* mice. (R) *Ob*/*ob* mice injected with Fc-CLEC2(ECD) show improvement in glucose tolerance 12 days after rAAV injection. (n = 12) *$p < 0.05$, **$p < 0.01$, ***$p < 0.001$, one-way ANOVA. Results are expressed as the mean ± SEM and are representative of three independent experiments, except (K) & (L) which are from one experiment.

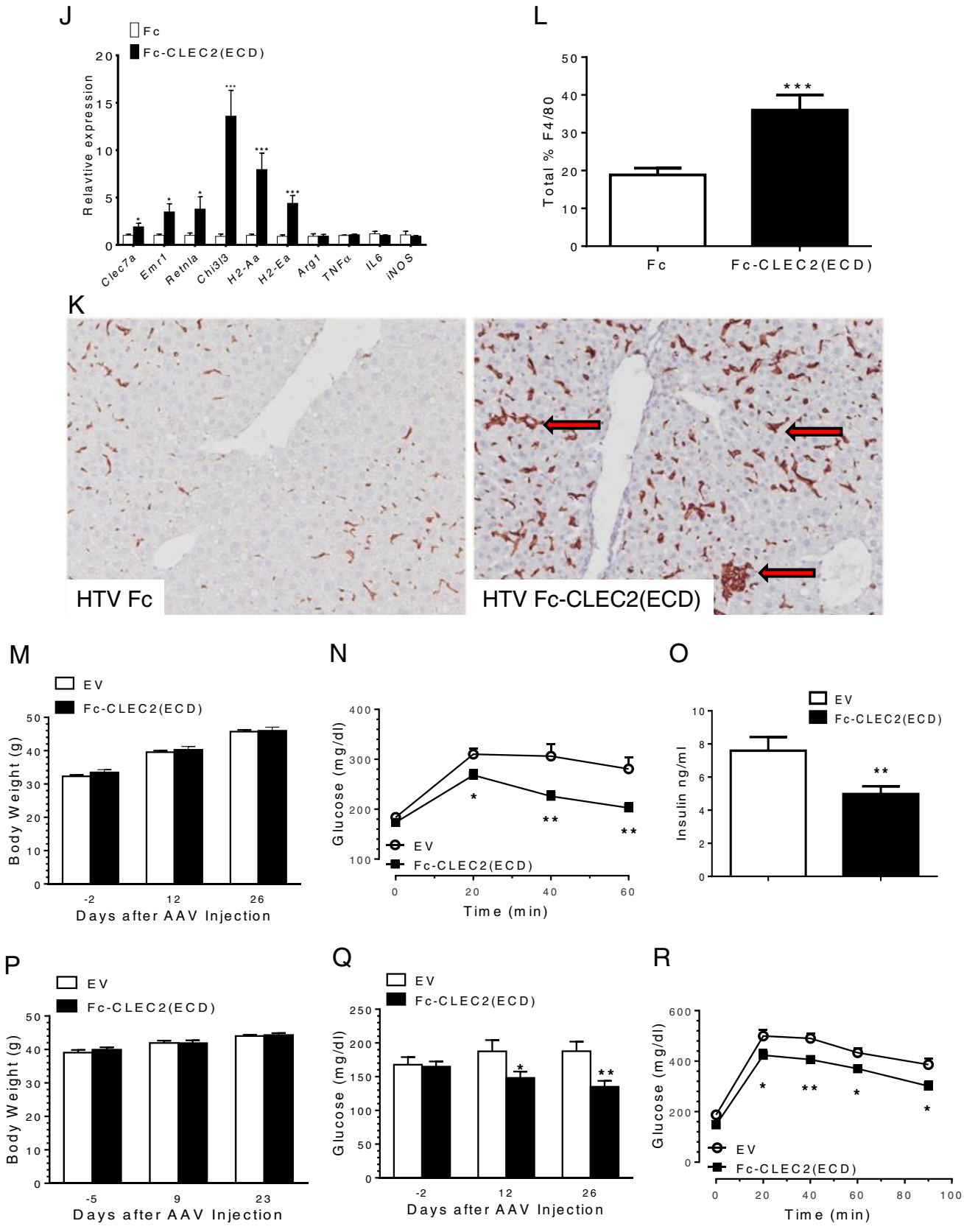

Fig. 2 (*continued*).

similar to that observed in the in vivo gene delivery experiments (Fig. 2). Also, no signs of fibrosis were found in livers as indicated by the negative immunohistochemical staining for αSMA (Supplementary Fig. 3A). Histopathological analysis of multiple organs, including the fat, skeletal muscle, and pancreas did not reveal any gross abnormalities in mice from treatment groups (Supplementary Fig. 3B).

3.5. Recombinant Fc-CLEC2(ECD) Simulates M2 Macrophage Activation in the Liver

Gene expression analysis was performed on livers from recombinant Fc-CLEC2(ECD) treated animals. Similar to animals treated by the gene delivery methods, markers of M2 macrophage activation, *Clec7a* and *Chi3l3*, were increased under the treatment conditions compared to the control group (Fig. 3F). Immunohistochemical staining with F4/80 to visualize Kupffer cells demonstrated a trending increase in F4/80+ staining area (Fig. 3H). As shown in Fig. 3G, treated mice also showed plumper Kupffer cells with some clusters surrounding liver fat vacuoles and some impinging on central vessels similar to HTV injected mice (Fig. 2K).

Since Kupffer cells are macrophages that clean up cell debris and endotoxin through phagocytosis, we measured several genes involved in phagocytosis, including *Coro1a*, *Ctss*, *Fcgr1* and *Itgb2*, all of which were induced in a dose dependent manner (Fig. 3F). Reduced macrophage phagocytic activity has been reported in several diabetes animal models (Liu et al., 1999; O'Brien et al., 2002) and hepatic phagocytic dysfunction has been associated with liver steatosis and abnormal cytokine regulation (Yang et al., 1997). Consistent with increased M2 macrophage markers in animals treated with soluble CLEC2, the level of the M2-associated anti-inflammatory cytokine, IL13, was increased (Fig. 3I). Moreover, several pro-inflammatory cytokines, G-CSF, KC and MIP-1a, were decreased in the serum (Fig. 3I) indicating that soluble CLEC2 stimulates Kupffer cell M2 activation and phagocytic activity, as well as suppresses the inflammation activity in diabetic animal models.

3.6. Activation of CLEC2 Suppresses M2 Macrophage Marker Expression In Vitro

To understand whether the observed induction of M2 markers in vivo is the direct action of Fc-CLEC2(ECD) on Kupffer cells or secondary to improvement in glucose metabolism, we explored the effects of CLEC2 on cultured RAW264.7 cells, a mouse leukemic monocyte macrophage cell line. To elucidate the effects of activating CLEC2 on macrophages, we utilized an agonistic anti-CLEC2 antibody confirmed by its ability to induce aggregation of platelets in vitro (Fig. 4A). Treatment of this anti-CLEC2 agonistic antibody on cultured RAW264.7 cells significantly suppressed the expression of the M2 marker, *Arg1*, but did not change the expression of the M1 marker, *Csf2*, suggesting that the activation of endogenous CLEC2 may suppress M2 activation in vitro (Fig. 4B). To further understand the possible physiological function of CLEC2, we isolated peritoneal macrophages from diabetic animals to examine *Clec2* expression. *Clec2* was highly expressed in *ob*/*ob* macrophages compared to wild type control animals while other *Clec* genes showed no difference between cohorts (Fig. 4C). These observations suggest that, under disease conditions, CLEC2 may contribute to increased inflammation, insulin resistance, and diabetes progression. Therefore, suppression of this pathway may lead to improvements in metabolic conditions. This is consistent with the observed improvements in glucose metabolism in animals treated with the soluble form of CLEC2 (Figs. 2 and 3), which could potentially act as a decoy receptor to antagonize endogenous receptor function.

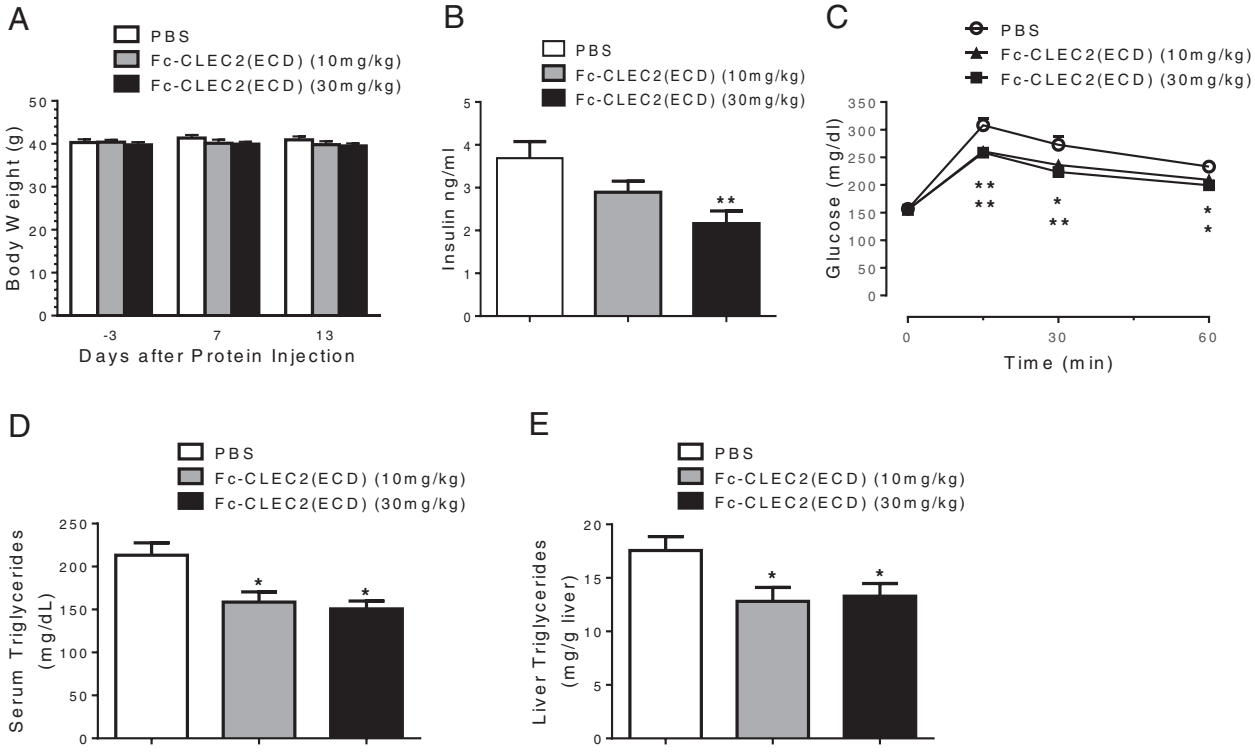

Fig. 3. Recombinant Fc-CLEC2(ECD) protein improved glucose homeostasis and hepatic steatosis. (A) Body weight comparison between DIO mice injected with recombinant Fc-CLEC2(ECD) protein and PBS control. (B) Recombinant Fc-CLEC2(ECD) protein reduces serum insulin concentration in DIO mice. (C) DIO mice injected with recombinant Fc-CLEC2(ECD) protein show improvement in glucose tolerance 7 days after first injection. (D) Recombinant Fc-CLEC2(ECD) protein reduces serum triglyceride concentration in DIO mice. (E) Liver triglyceride content is reduced in recombinant Fc-CLEC2(ECD) protein treated group. (n = 12) (F–I) Recombinant Fc-CLEC2(ECD) protein stimulates markers of M2 macrophages and phagocytosis in the liver and improves serum cytokine profile. (F) Up-regulation of liver macrophage and phagocytosis markers measured by RT-qPCR. (G) Liver macrophage F4/80 staining showing a wider distribution of plump clustered Kupffer cells in treated animals, with some clusters around degenerating hepatocytes and impinging on central veins, as indicated by arrows. (H) Quantification of liver macrophage F4/80 staining indicates a trended increase of F4/80+ staining in the Fc-CLEC2(ECD) treatment group. PBS control (n = 12), Fc-CLEC2(ECD) 10 mg/kg group (n = 12), Fc-CLEC2(ECD) 30 mg/kg group (n = 10). (I) Serum cytokine levels after recombinant Fc-CLEC2(ECD) protein treatment show increases in IL-13 and decreases in G-CSF, KC, and MIP-1a. $^{*}p < 0.05$, $^{**}p < 0.01$, $^{***}p < 0.001$, one-way ANOVA. Results are expressed as the mean ± SEM and are representative of two independent experiments.

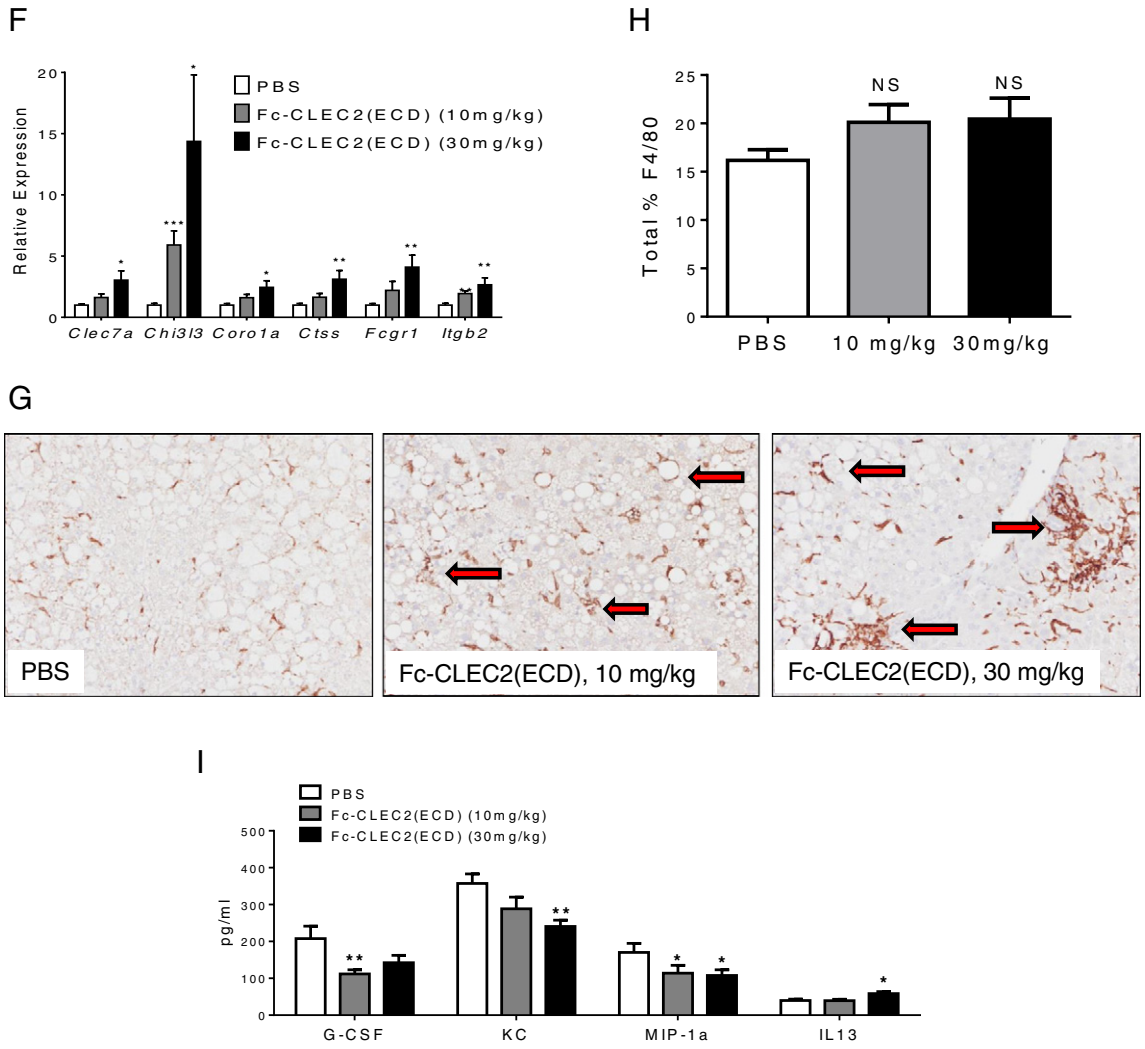

Fig. 3 (*continued*).

3.7. Fc-CLEC2(ECD) Simulates Liver Oxidative Phosphorylation and Fatty Acid Oxidation

To further explore the impact of CLEC2 function on Kupffer cells and hepatocytes, we examined expression of a panel of genes after treatment of co-cultured primary hepatocyte and Kupffer cells with soluble CLEC2. RT-qPCR analyses revealed a profound increase in the expression of oxidative phosphorylation genes, *Ndufs* and *Sdhb*, and enzymes for fatty acid beta-oxidation, *Acox1* and *Cpt1a*, but not the fatty acid transporter, *Slc27a1*. However, hepatocytes alone treated with soluble CLEC2 in the absence of Kupffer cells displayed no changes on these genes (data not shown) suggesting that activation of Kupffer cells by Fc-CLEC2(ECD) promotes oxidative metabolism in hepatocytes (Fig. 4D). Furthermore, activation of fatty acid oxidation may contribute to the observed reduction in liver TG in vivo upon Fc-CLEC2(ECD) treatment.

4. Discussion

Chronic inflammation, a hallmark feature of obesity and diabetes (Hotamisligil, 2006; Shoelson et al., 2006), is in part characterized by increased macrophage infiltration into adipose tissue, which in turn exacerbates insulin resistance (Weisberg et al., 2003; Xu et al., 2003). However, two distinct pathways for macrophage activation have been defined: pro-inflammatory M1 macrophages and anti-inflammatory M2 macrophages. Whereas M1 macrophages drive adipose inflammation in obese mice, macrophages residing in the adipose tissue of lean mice are predominantly of the M2 type and work to actively suppress inflammation (Lumeng et al., 2007a; Odegaard et al., 2007). Activation of liver-specific Kupffer cells contributes to liver steatosis and is also implicated in insulin resistance (Huang et al., 2010; Lanthier et al., 2010). Similar to adipose resident macrophages, Kupffer cells exhibit flexibility in that they can be activated toward either a classical pro-inflammatory state or an alternative anti-inflammatory state (Odegaard et al., 2008). Accordingly, alternatively activated M2-polarized Kupffer cells have been shown to ameliorate obesity-induced insulin resistance (Odegaard et al., 2008).

Although a role for the C-type lectin-like receptor, CLEC2, in platelet activation has been well described (Chang et al., 2010; Kerrigan et al., 2009; Mourao-Sa et al., 2011), a role for CLEC2 in immune cell function had yet to be elucidated. Among all tissues examined, we observed the highest expression of *Clec2* in the liver, presumably due to expression on the surface of Kupffer cells (Fig. 1C, Tang et al., 2010). Due to the lack of known endogenous ligands for CLEC2, we chose to focus on a loss-of-function study using the soluble CLEC2 ECD as a potential dominant negative factor to block endogenous CLEC2 receptor function. Using this approach, our results were consistent across all models tested and revealed that Fc-CLEC2(ECD) treatment can reproducibly induce markers of alternatively activated Kupffer cells, including *Clec7a*, *Retnla*,

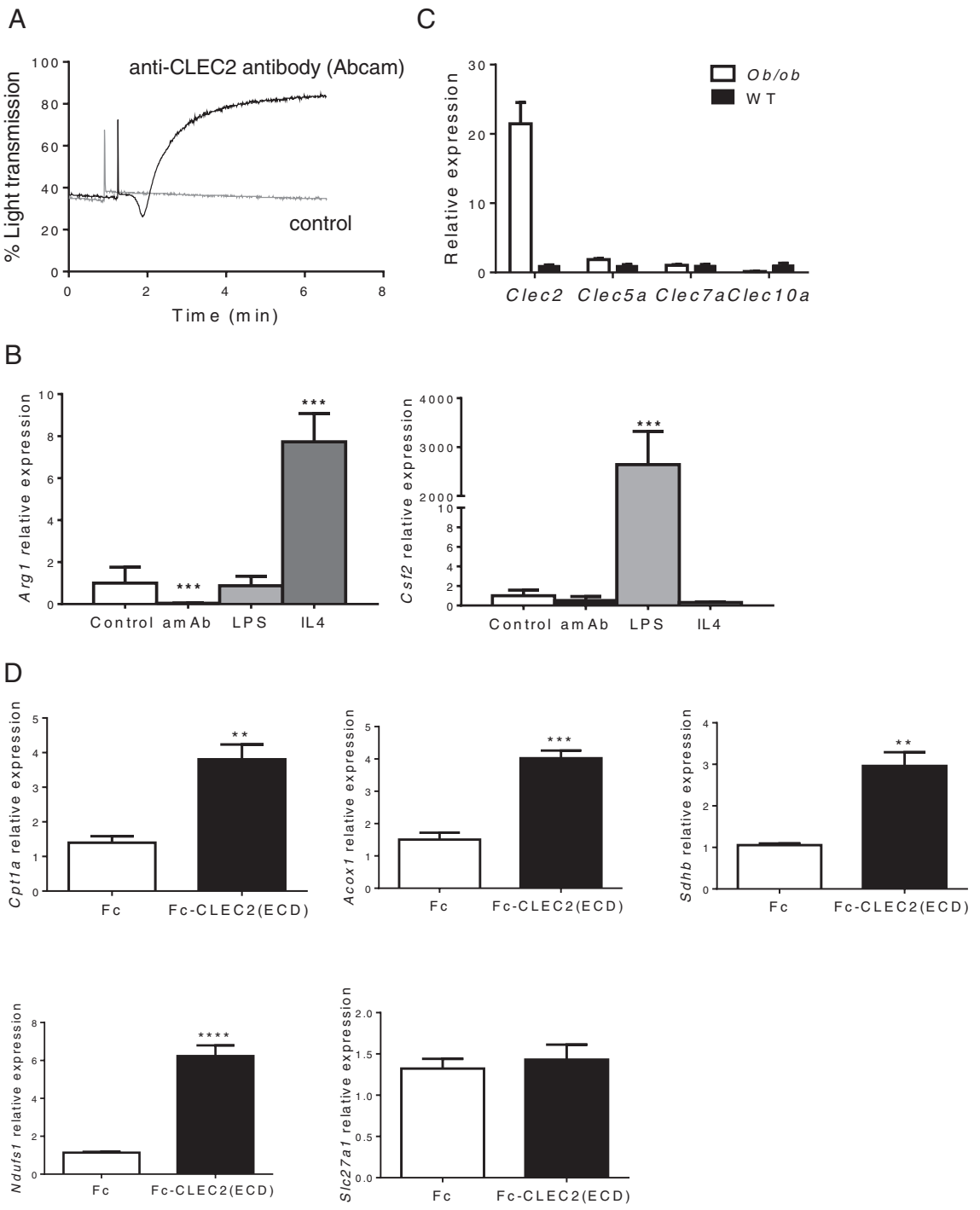

Fig. 4. Effects of CLEC2 in vitro. (A–C) Activation of CLEC2 suppresses markers for M2 lineage of macrophage in vitro. (A) Anti-CLEC2 agonistic antibody induces strong aggregation of platelets. (B) Cultured RAW264.7 cells, treated with the CLEC2 agonistic antibody for 24 h, show significantly suppressed M2 marker, *Arg1*, but not M1 marker, *Csf2*. Antibody at 10 nM, LPS at 1 μg/ml, and IL4 at 100 ng/ml. amAb represents agonistic CLEC2 antibody. (C) Isolated peritoneal macrophages from 6 week old *ob*/*ob* animals show high expression of *Clec2* but not other *Clec* molecules such as *Clec5a*, *Clec7a*, and *Clec10a* (***$p < 0.001$). (D) Fc-CLEC2(ECD) simulates liver oxidative phosphorylation and fatty acid oxidation in co-cultured Kupffer cells and primary hepatocytes. Co-cultured Kupffer cells and primary hepatocytes were treated with Fc-CLEC2(ECD) at a concentration of 200 ng/ml for 5 h. Fc-CLEC2(ECD) treatment induces expression of genes encoding components of oxidative phosphorylation (*Ndufs*, *Sdhb*) and fatty acid beta-oxidation (*Acox1*, *Cpt1a*), but not fatty acid transporters (*Slc27a1*). *$p < 0.05$, **$p < 0.01$, ***$p < 0.001$, one-way ANOVA. Results are expressed as the mean ± SEM and are representative of four independent experiments.

and *Chi313*, and significantly improved glucose and lipid metabolism. These results suggest that the endogenous CLEC2 receptor may play a pro-inflammatory role under disease conditions which is consistent with the observation that *Clec2* expression in macrophages of diabetic animals is dramatically increased. Gene expression profiling further showed that Fc-CLEC2(ECD) stimulates a phagocytic activity in the liver. The liver has a highly developed filtering mechanism to maintain homeostasis in the circulation and Kupffer cells are key players in this process (Toth and Thomas, 1992). The Kupffer cells form a protective barrier for the systemic circulation and remove many harmful materials such as endotoxins and cellular debris through phagocytosis (Toth and Thomas, 1992). It is known that under diabetic and metabolic syndrome conditions, macrophages display altered immune activities such as decreased phagocytosis due to insulin resistance (Liang et al., 2007;

Plotkin et al., 1996), and that dysfunction of the phagocytic activity can result in the accumulation of materials that cause inflammatory responses and exacerbate insulin resistance. Our results suggest that Fc-CLEC2(ECD) improves the deficiency in Kupffer cell phagocytosis present under diseased conditions, reduces pro-inflammatory cytokine release, and increases anti-inflammatory cytokine production. Given the important role played by inflammation in insulin resistance and metabolic disorders, our data suggests that the anti-inflammatory activity of Fc-CLEC2(ECD) contributes to the improvement of glucose and lipid metabolism observed in our studies.

Although the physiological role of CLEC2 in Kupffer cell activation and phagocytic activity is not completely understood, published studies support our hypothesis. Kerrigan et al., for example, generated a chimeric receptor bearing the extracellular and transmembrane domains of CLEC7a and the cytoplasmic tail of CLEC2 to investigate CLEC2 function on neutrophils (Kerrigan et al., 2009). Whether the capacity of the chimeric protein, when expressed in cell lines, reflects the actual endogenous function of an intact CLEC2 receptor was not resolved, but the results indicated that the cytoplasmic tail of CLEC2, at least, could mediate a phagocytic activity. In another series of studies, Chang et al. (2010) showed that rhodocytin specifically induced macrophage secretion of proinflammatory cytokines, and Mourao-Sa et al. (2011) demonstrated that cross-linking of an anti-CLEC2 agonistic antibody in myeloid cell cultures modulated the effects of toll-like receptor (TLR) agonists to potentiate anti-proinflammatory IL-10 production. Thus, several published reports point toward a role for CLEC2 in macrophage function.

To further understand the potential mechanism leading to the improved glucose and lipid homeostasis observed, we performed studies with co-cultured Kupffer cells and hepatocytes. Our results demonstrate that treatment of the co-culture with soluble CLEC2 improves measures of liver oxidative phosphorylation and fatty acid oxidation. These data suggest that hepatocytes may be a source of an endogenous ligand for CLEC2. Furthermore, the local paracrine loop between hepatocytes and Kupffer cells may also contribute to the improvements we observed in hepatosteatosis when diseased mice were given Fc-CLEC2(ECD) treatment.

Although the results suggest that liver Kupffer cells are a potential target for Fc-CLEC2(ECD)-mediated suppression of inflammation and subsequent improvement of metabolic parameters, it remains possible that this effect is indirect. In addition, it is important to note that there may be additional Fc-CLEC2(ECD) targets. CLEC2 is expressed on the surface of many myeloid cells including dendritic cells and neutrophils (Mourao-Sa et al., 2011), thus, whether the improved metabolic phenotypes induced by Fc-CLEC2(ECD) are due to its effects on the function of CLEC2 receptor on those cells, or due to a gain-of-function effect independent of the CLEC2 receptor, will require additional investigation.

In summary, using multiple in vitro and in vivo approaches we identified a previously unknown connection between CLEC2 and Kupffer cell activation. Our results demonstrate that the extracellular domain of CLEC2 improves glucose homeostasis and hepatic steatosis in diabetic mouse models. Our data support that targeting CLEC2 may be a promising new strategy for developing therapies for treating diabetes and possibly steatotic liver diseases.

Author Contributions

X.W., J.Z., H.G., J.Gupte, H.B., K.J.L., B.L., S.C., Y.G., Z.P., I.C.R., and J.Gardner performed experiments; X.W., J.Z., H.G., J.Gupte, H.B., S.C., Z.P., I.C.R., W.G.R., and Y.L. analyzed and interpreted data; X.W., J.Z., W.G.R., and Y.L. designed the research; X.W., J.Z., and Y.L. wrote the manuscript and I.C.R. edited the manuscript.

Conflict of Interest

This work was funded by Amgen Inc. All authors were full time Amgen employees when the work was performed.

Acknowledgments

The authors thank Tom Wolfe, Huiren Zhao, Jiangwen Majeti, Xiong Gao, Li Yang, Jay Tang, and Kim Samayoa for technical assistance. We thank Wen-Chen Yeh, Gene Cutler, Richard Smith, and Scott Simonet for helpful discussions and critical review of the manuscript.

Appendix A. Supplementary data

Supplementary data to this article can be found online at http://dx.doi.org/10.1016/j.ebiom.2015.02.013.

References

Bertozzi, C.C., Hess, P.R., Kahn, M.L., 2010. Platelets: covert regulators of lymphatic development. Arterioscler. Thromb. Vasc. Biol. 30, 2368–2371.
Chang, C.H., Chung, C.H., Hsu, C.C., Huang, T.Y., Huang, T.F., 2010. A novel mechanism of cytokine release in phagocytes induced by aggretin, a snake venom C-type lectin protein, through CLEC-2 ligation. J. Thromb. Haemost. 8, 2563–2570.
Charo, I.F., 2007. Macrophage polarization and insulin resistance: PPARgamma in control. Cell Metab. 6, 96–98.
Christou, C.M., Pearce, A.C., Watson, A.A., Mistry, A.R., Pollitt, A.Y., Fenton-May, A.E., Johnson, L.A., Jackson, D.G., Watson, S.P., O'Callaghan, C.A., 2008. Renal cells activate the platelet receptor CLEC-2 through podoplanin. Biochem. J. 411, 133–140.
Colonna, M., Samaridis, J., Angman, L., 2000. Molecular characterization of two novel C-type lectin-like receptors, one of which is selectively expressed in human dendritic cells. Eur. J. Immunol. 30, 697–704.
Gordon, S., Taylor, P.R., 2005. Monocyte and macrophage heterogeneity. Nat. Rev. Immunol. 5, 953–964.
Harkins, J.M., Moustaid-Moussa, N., Chung, Y.J., Penner, K.M., Pestka, J.J., North, C.M., Claycombe, K.J., 2004. Expression of interleukin-6 is greater in preadipocytes than in adipocytes of 3T3-L1 cells and C57BL/6J and ob/ob mice. J. Nutr. 134, 2673–2677.
Hevener, A.L., Olefsky, J.M., Reichart, D., Nguyen, M.T., Bandyopadyhay, G., Leung, H.Y., Watt, M.J., Benner, C., Febbraio, M.A., Nguyen, A.K., et al., 2007. Macrophage PPAR gamma is required for normal skeletal muscle and hepatic insulin sensitivity and full antidiabetic effects of thiazolidinediones. J. Clin. Invest. 117, 1658–1669.
Hooley, E., Papagrigoriou, E., Navdaev, A., Pandey, A.V., Clemetson, J.M., Clemetson, K.J., Emsley, J., 2008. The crystal structure of the platelet activator aggretin reveals a novel (alphabeta)2 dimeric structure. Biochemistry 47, 7831–7837.
Hotamisligil, G.S., 2006. Inflammation and metabolic disorders. Nature 444, 860–867.
Huang, W., Metlakunta, A., Dedousis, N., Zhang, P., Sipula, I., Dube, J.J., Scott, D.K., O'Doherty, R.M., 2010. Depletion of liver Kupffer cells prevents the development of diet-induced hepatic steatosis and insulin resistance. Diabetes 59, 347–357.
Kang, K., Reilly, S.M., Karabacak, V., Gangl, M.R., Fitzgerald, K., Hatano, B., Lee, C.H., 2008. Adipocyte-derived Th2 cytokines and myeloid PPARdelta regulate macrophage polarization and insulin sensitivity. Cell Metab. 7, 485–495.
Kato, Y., Kaneko, M.K., Kunita, A., Ito, H., Kameyama, A., Ogasawara, S., Matsuura, N., Hasegawa, Y., Suzuki-Inoue, K., Inoue, O., et al., 2008. Molecular analysis of the pathophysiological binding of the platelet aggregation-inducing factor podoplanin to the C-type lectin-like receptor CLEC-2. Cancer Sci. 99, 54–61.
Kerrigan, A.M., Dennehy, K.M., Mourao-Sa, D., Faro-Trindade, I., Willment, J.A., Taylor, P.R., Eble, J.A., Reis e Sousa, C., Brown, G.D., 2009. CLEC-2 is a phagocytic activation receptor expressed on murine peripheral blood neutrophils. J. Immunol. 182, 4150–4157.
Lanthier, N., Molendi-Coste, O., Horsmans, Y., van Rooijen, N., Cani, P.D., Leclercq, I.A., 2010. Kupffer cell activation is a causal factor for hepatic insulin resistance. Am. J. Physiol. Gastrointest. Liver Physiol. 298, G107–G116.
Li, Z., Diehl, A.M., 2003. Innate immunity in the liver. Curr. Opin. Gastroenterol. 19, 565–571.
Liang, C.P., Han, S., Senokuchi, T., Tall, A.R., 2007. The macrophage at the crossroads of insulin resistance and atherosclerosis. Circ. Res. 100, 1546–1555.
Liu, B.F., Miyata, S., Kojima, H., Uriuhara, A., Kusunoki, H., Suzuki, K., Kasuga, M., 1999. Low phagocytic activity of resident peritoneal macrophages in diabetic mice: relevance to the formation of advanced glycation end products. Diabetes 48, 2074–2082.
Lumeng, C.N., Saltiel, A.R., 2011. Inflammatory links between obesity and metabolic disease. J. Clin. Invest. 121, 2111–2117.
Lumeng, C.N., Bodzin, J.L., Saltiel, A.R., 2007a. Obesity induces a phenotypic switch in adipose tissue macrophage polarization. J. Clin. Invest. 117, 175–184.
Lumeng, C.N., Deyoung, S.M., Bodzin, J.L., Saltiel, A.R., 2007b. Increased inflammatory properties of adipose tissue macrophages recruited during diet-induced obesity. Diabetes 56, 16–23.
Mantovani, A., Sozzani, S., Locati, M., Allavena, P., Sica, A., 2002. Macrophage polarization: tumor-associated macrophages as a paradigm for polarized M2 mononuclear phagocytes. Trends Immunol. 23, 549–555.
Mjosberg, J.M., Trifari, S., Crellin, N.K., Peters, C.P., van Drunen, C.M., Piet, B., Fokkens, W.J., Cupedo, T., Spits, H., 2011. Human IL-25- and IL-33-responsive type 2 innate lymphoid cells are defined by expression of CRTH2 and CD161. Nat. Immunol. 12, 1055–1062.
Mourao-Sa, D., Robinson, M.J., Zelenay, S., Sancho, D., Chakravarty, P., Larsen, R., Plantinga, M., Van Rooijen, N., Soares, M.P., Lambrecht, B., et al., 2011. CLEC-2 signaling via Syk in myeloid cells can regulate inflammatory responses. Eur. J. Immunol. 41, 3040–3053.

National Research Council (U.S.). Committee for the Update of the Guide for the Care and Use of Laboratory Animals, Institute for Laboratory Animal Research (U.S.), National Academies Press (U.S.), 2011. Guide for the Care and Use of Laboratory Animals. National Academies Press, Washington, D.C., p. xxv (220 pp.).

O'Brien, B.A., Huang, Y., Geng, X., Dutz, J.P., Finegood, D.T., 2002. Phagocytosis of apoptotic cells by macrophages from NOD mice is reduced. Diabetes 51, 2481–2488.

Odegaard, J.I., Ricardo-Gonzalez, R.R., Goforth, M.H., Morel, C.R., Subramanian, V., Mukundan, L., Red Eagle, A., Vats, D., Brombacher, F., Ferrante, A.W., et al., 2007. Macrophage-specific PPARgamma controls alternative activation and improves insulin resistance. Nature 447, 1116–1120.

Odegaard, J.I., Ricardo-Gonzalez, R.R., Red Eagle, A., Vats, D., Morel, C.R., Goforth, M.H., Subramanian, V., Mukundan, L., Ferrante, A.W., Chawla, A., 2008. Alternative M2 activation of Kupffer cells by PPARdelta ameliorates obesity-induced insulin resistance. Cell Metab. 7, 496–507.

Plotkin, B.J., Paulson, D., Chelich, A., Jurak, D., Cole, J., Kasimos, J., Burdick, J.R., Casteel, N., 1996. Immune responsiveness in a rat model for type II diabetes (Zucker rat, fa/fa): susceptibility to *Candida albicans* infection and leucocyte function. J. Med. Microbiol. 44, 277–283.

Shoelson, S.E., Lee, J., Goldfine, A.B., 2006. Inflammation and insulin resistance. J. Clin. Invest. 116, 1793–1801.

Sobanov, Y., Bernreiter, A., Derdak, S., Mechtcheriakova, D., Schweighofer, B., Duchler, M., Kalthoff, F., Hofer, E., 2001. A novel cluster of lectin-like receptor genes expressed in monocytic, dendritic and endothelial cells maps close to the NK receptor genes in the human NK gene complex. Eur. J. Immunol. 31, 3493–3503.

Steinman, R.M., Idoyaga, J., 2010. Features of the dendritic cell lineage. Immunol. Rev. 234, 5–17.

Suzuki-Inoue, K., Fuller, G.L., Garcia, A., Eble, J.A., Pohlmann, S., Inoue, O., Gartner, T.K., Hughan, S.C., Pearce, A.C., Laing, G.D., et al., 2006. A novel Syk-dependent mechanism of platelet activation by the C-type lectin receptor CLEC-2. Blood 107, 542–549.

Suzuki-Inoue, K., Kato, Y., Inoue, O., Kaneko, M.K., Mishima, K., Yatomi, Y., Yamazaki, Y., Narimatsu, H., Ozaki, Y., 2007. Involvement of the snake toxin receptor CLEC-2, in podoplanin-mediated platelet activation, by cancer cells. J. Biol. Chem. 282, 25993–26001.

Tang, T., Li, L., Tang, J., Li, Y., Lin, W.Y., Martin, F., Grant, D., Solloway, M., Parker, L., Ye, W., et al., 2010. A mouse knockout library for secreted and transmembrane proteins. Nat. Biotechnol. 28, 749–755.

Toth, C.A., Thomas, P., 1992. Liver endocytosis and Kupffer cells. Hepatology 16, 255–266.

Weisberg, S.P., McCann, D., Desai, M., Rosenbaum, M., Leibel, R.L., Ferrante Jr., A.W., 2003. Obesity is associated with macrophage accumulation in adipose tissue. J. Clin. Invest. 112, 1796–1808.

Xu, H., Barnes, G.T., Yang, Q., Tan, G., Yang, D., Chou, C.J., Sole, J., Nichols, A., Ross, J.S., Tartaglia, L.A., et al., 2003. Chronic inflammation in fat plays a crucial role in the development of obesity-related insulin resistance. J. Clin. Invest. 112, 1821–1830.

Yang, S.Q., Lin, H.Z., Lane, M.D., Clemens, M., Diehl, A.M., 1997. Obesity increases sensitivity to endotoxin liver injury: implications for the pathogenesis of steatohepatitis. Proc. Natl. Acad. Sci. U. S. A. 94, 2557–2562.